Strong Coupling in a Microcavity LED

Jonathan R. Tischler,* M. Scott Bradley,* and Vladimir Bulović†
Massachusetts Institute of Technology, Cambridge, Massachusetts 02139, USA

Jung Hoon Song and Arto Nurmikko
Division of Engineering and Department of Physics, Brown University, Providence, Rhode Island 02912, USA
(Received 4 February 2005; published 15 July 2005)

Thin films of polyelectrolyte/*J* aggregate dye bilayers with high absorption coefficient (6 nm thick with $\alpha \approx 1.0 \times 10^6$ cm^{-1}) inserted in an optical microcavity enable the cavity quantum electrodynamic strong coupling limit to be reached at room temperature with a coupling strength (Rabi splitting) of 265 ± 15 meV. By embedding these films in a resonant cavity organic LED structure, we demonstrate the first emissive electrically pumped exciton-polariton device.

DOI: 10.1103/PhysRevLett.95.036401 PACS numbers: 71.36.+c, 71.35.Aa, 85.60.Jb

The strong coupling limit of cavity QED is reached when matter inserted inside a microcavity exchanges energy with the resonant mode of the cavity more rapidly than the combined rate at which light leaves the cavity and the matter wave function loses its phase information [1,2]. In this limit, the microcavity and matter form a composite quantum system with two new eigenstates that are superpositions of the initial uncoupled states, with new eigenenergies separated in energy by the Rabi splitting. The matter component of the coupled system can be a gas of atoms trapped inside the cavity [3], a superconducting qubit [4], or a solid state thin film containing excitons, in the form of an inorganic quantum well [5], quantum dot [6,7], or organic material [8], in which case the superposition states are referred to as exciton polaritons. Applications of strong coupling in atomic and semiconductor systems have led to one-atom zero threshold lasers [9], high gain polariton parametric amplifiers [10], and predictions that strong coupling may play a key role in future quantum information processors [11]. These experiments have all relied on optical pumping. Here we demonstrate electrically pumped exciton-polariton emission, the first device in which strongly coupled states of light and matter are electrically excited.

The matter component of our device is a 6 ± 1 nm thick film of *J* aggregated dye. The film consists of 4 bilayers [12] of the cationic polyelectrolyte PDAC (poly diallyldimethylammonium chloride) and *J* aggregates of the anionic cyanine dye TDBC (5,6-dichloro-2-[3-[5,6-dichloro-1-ethyl-3-(3-sulfopropyl)-2(3H)-benzimidazolidene]-1-propenyl]-1-ethyl-3-(3-sulfopropyl) benzimidazolium hydroxide, inner salt, sodium salt), molecular structures shown in Fig. 1(a). The *J* aggregates are crystallites of dye in which the transition dipoles of the constituent molecules strongly couple to form a collective narrow linewidth optical transition possessing oscillator strength derived from all the aggregated monomers [13]. The bilayer films contain a high density of *J* aggregated TDBC and therefore have a very large peak absorption constant ($\alpha \approx 1.0 \times 10^6$ cm^{-1}) [14].

We reach the strong coupling limit by embedding the PDAC/TDBC films in the resonant cavity organic light emitting device (RC-OLED) described in Fig. 1(b). The microcavity is formed by the two Ag electrodes. Although the quality of the resonator is only $Q \approx 10$, because of losses from the metal mirrors, strong coupling is still reached [15] due to the high absorption of the PDAC/TDBC films. To enable electrical excitation of the *J* aggregates, the PDAC/TDBC film is sandwiched between wider band-gap poly-TPD [poly(N,N′-bis(4-butylphenyl-N,N′-bis(phenyl)benzidine)] and BCP (2,9-Dimethyl-4,7-diphenyl-1,10-phenanthroline) layers, hole and electron transporting, respectively, akin to a *p-i-n* LED design [16]. A typical device is between 112 and 135 nm thick, not including the metal mirror thicknesses, with 0.1 A cm^{-2} current density reached at 10 V applied bias.

The RC-OLEDs exhibit strong coupling when electrically excited, with the exciton-polariton electroluminescence (EL) peaks observed at room temperature. The exciton-polariton peaks in EL and dips in reflectivity spectra are most pronounced when the microcavity is resonantly tuned to the TDBC peak reflection wavelength $\lambda = 595$ nm. The observed room temperature Rabi splitting between exciton-polariton peaks is 265 ± 15 meV, an order of magnitude larger than in inorganic quantum well structures [17], which is a consequence [2] of the high absorption coefficient of the PDAC/TDBC films.

Spectral properties of the RC-OLEDs noticeably differ from the spectra of an uncoupled OLED [18], one with the same organic layer thicknesses but without the 50 nm Ag mirror. For the RC-OLED with 54 nm thick poly-TPD film, the reflectance [Fig. 1(c)] spectrum exhibits two resonant dips at $\lambda = 554$ nm and $\lambda = 625$ nm. In contrast, the 4 bilayers of PDAC/TDBC on glass have a single resonance at $\lambda = 595$ nm (FWHM = 19 nm), and the bare microcavity would produce a resonant dip at $\lambda = 587$ nm. Similarly, in EL [Fig. 2(c)], the forward ($\theta = 0°$) spectrum of the uncoupled OLED has one emission peak at $\lambda = 602$ nm (FWHM = 23 nm), corresponding to the resonance of the uncoupled TDBC *J* aggregate exciton,

while in the RC-OLED, the single emission peak splits into two peaks located at $\lambda = 546$ nm and $\lambda = 622$ nm.

The large splitting between the resonances of the Fig. 1(c) RC-OLED is due to strong coupling between the J aggregate exciton ($\lambda = 595$ nm) and the photon field of the near resonantly tuned microcavity ($\lambda = 587$ nm). Because of the strong coupling, the exciton and photon are exchanging energy at a faster rate than the respective dephasing processes, namely, dephasing due to spontaneous emission and nonradiative relaxation of the J aggregate exciton and photon dephasing due to light leakage from the cavity [1,2]. Consequently, new eigenstates form with

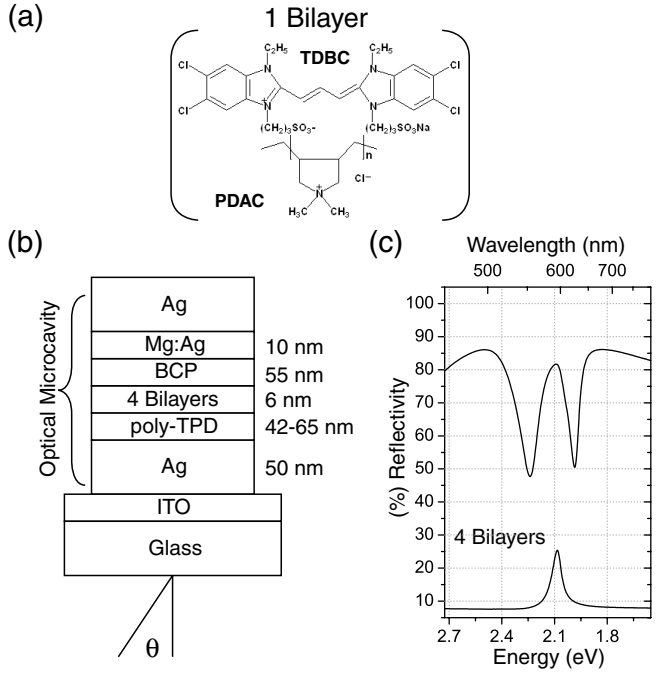

FIG. 1. (a) Chemical structure of PDAC/TDBC bilayer containing the cationic polyelectrolyte PDAC and anionic TDBC, a J aggregate forming cyanine dye. To assemble a bilayer, a substrate is immersed in 20% (w/v) PDAC solution in deionized water (DI) for 15 min, and then rinsed 3 times with DI (2, 2, and 1 min) to remove all but the first monolayer of PDAC. The substrate is then immersed into 50 μM, pH 9.0, TDBC solution for 15 min, followed by three additional rinses (pH 9.0, 2 min, 2 min, and 1 min) to remove excess dye. The process is repeated to assemble multiple bilayers. (b) Resonant cavity organic light emitting device (RC-OLED) structure, with variable thickness spin-cast poly-TPD layer that tunes microcavity resonance. The substrate consists of precleaned indium tin oxide (ITO) coated glass. Metal layers dually serve as mirrors for the microcavity and as electrical contacts to the device. The 50 nm anodic mirror is semitransparent, allowing for light collection through the substrate side of the device. A 10 nm Mg:Ag alloy layer facilitates electron injection from the cathode into the organic layers. (c) Reflectivity of RC-OLED with poly-TPD thickness of 54 nm, compared to 4 bilayer film on glass, measured at $\theta = 7°$. The microcavity is tuned to $\lambda = 587$ nm, near resonant with the TDBC J aggregate peak at $\lambda = 595$ nm.

energy levels, $E_{\pm}$, separated from the uncoupled exciton and photon energy levels, E_{ex} and E_{ph}, respectively,

$$E_{\pm} = \frac{E_{\mathrm{ex}} + E_{\mathrm{ph}}}{2} \pm \frac{1}{2}\sqrt{(\hbar\Omega_i)^2 + (E_{\mathrm{ex}} - E_{\mathrm{ph}})^2}. \quad (1)$$

The energy separation, $E_+ - E_-$, is dependent on the degree of energy matching between the exciton and photon modes, and has a minimum of $\hbar\Omega_i$ when the exciton and photon are resonant, $E_{\mathrm{ex}} = E_{\mathrm{ph}}$. $\hbar\Omega_i$ is the exciton-photon vacuum Rabi coupling frequency, which increases with the strength of the exciton-photon interaction [2].

The dependence of polariton energy levels $E_{\pm}$ on E_{ph} described by Eq. (1) is evidenced in Fig. 2, which plots EL and reflectivity in the normal direction for multiple RC-OLEDs with different microcavity thicknesses. As the poly-TPD layer thickness is varied from 65 to 42 nm, E_{ph} is tuned between 1.98 and 2.26 eV, spanning the energy range that encompasses the J aggregate exciton resonance, $E_{\mathrm{ex}} = 2.08$ eV ($\lambda = 595$ nm). As a result, the energy separation between resonant dips in reflectivity varies from more than 300 meV [Fig. 2(b)], when the exciton and photon are far off resonance to a minimum of $\hbar\Omega_i = 265$ meV, when $E_{\mathrm{ex}} = E_{\mathrm{ph}}$, which corresponds to a thickness of 56 nm for the poly-TPD layer. Similarly in EL, the $E_{\pm}$ spectral peaks [Figs. 2(c) and 2(d)] are greatly separated off resonance and then approach each other as the microcavity is tuned through E_{ex}.

In the EL of Fig. 2(c), a spectral shoulder at $\lambda = 610$ nm appears superimposed on the emission spectrum of the E_- state. This emission could be from J aggregates that are not strongly coupled to the microcavity due to disorder in the bilayers. The shoulder is absent in reflectivity [Fig. 2(a)] because optical excitation selects the J aggregates with transition dipoles oriented parallel to the mirrors and therefore only J aggregates contributing to strong coupling are excited.

The characteristic dependence of $E_{\pm}$ on E_{ph} is also observed in the angular EL spectra of the RC-OLEDs, since changing θ affects the tuning of E_{ph}. As θ increases, E_{ph} tunes towards higher energy according to the dispersion relation [2]:

$$E_{\mathrm{ph}}(\theta) = E_0(1 - \sin^2\theta/n^2)^{-1/2}, \quad (2)$$

where E_0 is the bare cavity resonance at $\theta = 0°$ and n is the refractive index of the cavity spacer layers. E_{ex}, however, remains constant. In particular, for the RC-OLED of Fig. 1(c), $E_{\mathrm{ph}}(\theta = 0°) = 2.11$ eV, while $E_{\mathrm{ph}}(\theta = 80°) = 2.59$ eV (with $n = 1.7$ for the poly-TPD and BCP layers). Figures 3(a)–3(c) plot the angular reflectivity and EL spectra for this RC-OLED.

As a result of the angular dependence, the polariton energy levels of Eq. (1) become functions of θ with $E_{\pm} \rightarrow E_{\pm}(\theta)$. Figure 3(d) plots the angular dependence of the EL peaks and reflectivity dips together with the calculated dispersion relations for $E_{\mathrm{ph}}(\theta)$ and the polariton states

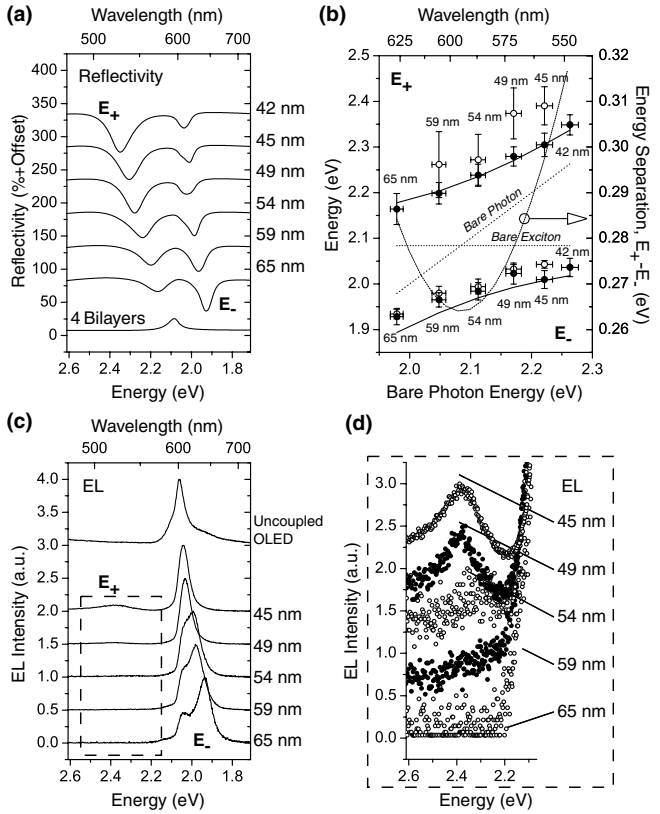

FIG. 2. Normal mode polariton electroluminescence and reflectivity for a series of RC-OLED structures with different microcavity resonances. Cavity resonance is tuned across a 250 meV band, by adjusting the thickness of the poly-TPD layer from 42 to 65 nm. (a) Reflectivity at $\theta = 7°$ for a series of RC-OLED structures. Data of successive measurements are offset by 50 percentage points. The reflectivity of a 4 bilayer PDAC/TDBC film is shown for comparison. (b) Resonant peaks in EL (open data points) and resonant dips in reflectivity (solid data points) plotted as a function of the bare (cavity) photon energy exhibit anticrossing. Fits are generated by the two-state model of Eq. (1), with a Rabi splitting of $\hbar\Omega_i = 265$ meV. (c) EL spectra at $\theta = 0°$, normalized to the lowest energy peak, E_-. The spectral shoulder at $\lambda = 610$ nm is EL from disordered J aggregates not strongly coupled to cavity. (d) Expanded view of high-energy portion of EL spectra, normalized to emission of the higher energy polariton peak, E_+, in the $\lambda = 475$ to 575 nm range.

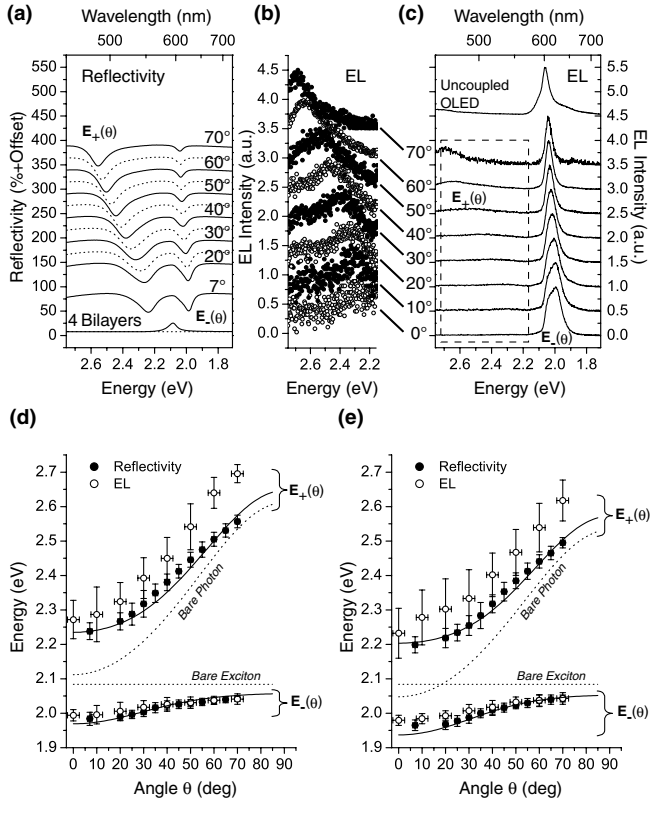

FIG. 3. Angularly resolved polariton electroluminescence and reflectivity measurements for the polariton RC-OLED of Fig. 2 with poly-TPD thickness of 54 nm, and dispersion relations in (d) and (e) for RC-OLEDs with poly-TPD thicknesses of 54 and 59 nm, respectively. (a) TE polarized reflectivity. Data of successive measurements are offset by 50 percentage points. The reflectivity at $\theta = 7°$ of a 4 bilayer PDAC/TDBC film is shown for comparison. (b) Expanded view of a higher energy portion of the EL spectra, normalized to emission of the higher energy polariton peak, $E_+(\theta)$, in the $\lambda = 450$ to 575 nm range. (c) EL spectra normalized to lower energy polariton peak, $E_-(\theta)$. The EL spectrum at $\theta = 0°$ of an uncoupled OLED is shown for comparison. (d) Polariton angular dispersion relation for RC-OLED of parts (a)–(c) with $E_{\rm ph}(\theta = 0°) = 2.11$ eV. The fit is generated from reflectivity data in (a) using the two-state model of Eq. (1), with the coupling interaction, $\hbar\Omega_i = 265$ meV, being independent of angle and the bare (cavity) photon energy following Eq. (2). (e) Polariton angular dispersion relation for RC-OLED with $E_{\rm ph}(\theta = 0°) = 2.05$ eV, and fit with $\hbar\Omega_i = 265$ meV.

$E_\pm(\theta)$. At $\theta = 0°$, near resonance for $E_{\rm ph}(\theta)$ and $E_{\rm ex}$, the polariton branches of the dispersion relation $E_\pm(\theta)$ anticross in energy, while at larger θ, far away from the resonance condition, they devolve into uncoupled exciton and photon dispersion curves. The EL spectra of Figs. 2(c) and 3(c) show that the intensity of the upper branch, $E_+(\theta)$, is significantly attenuated compared to that of the lower branch, $E_-(\theta)$, in contrast to reflectivity [Figs. 1(c), 2(a), and 3(a)] where the resonant dips are of similar magnitude. Thermalization of the polaritons account for the lower intensity of E_+ in the EL spectra.

A single value for the vacuum Rabi splitting, $\hbar\Omega_i = 265$ meV, is used to generate the fits in Figs. 2(b) and 3(d) and also Fig. 3(e), which plots the angular dispersion of the RC-OLED with $E_{\rm ph}(\theta = 0°) = 2.05$ eV (poly-TPD thickness of 59 nm in Fig. 2). Consistent agreement of the RC-OLED data, across multiple devices and collection angles, with a single value of $\hbar\Omega_i$ in the dispersion relation defined by Eq. (1), further confirms that the RC-OLEDs operate in the strong coupling limit.

EL and reflectivity measurements yield similar dispersion relations, as they are both linear optical probes of the polariton energy levels, confirming that electrical excitation, at the applied field ($\approx 10^6$ V cm^{-1}) and current density (≈ 0.1 A cm^{-2}), does not change the optical energy levels of the polariton states. The applied field does not perturb the Rabi splitting since the dipoles contributing most to strong coupling lay in the plane perpendicular to the direction of the applied E field.

Although the dispersion relations mostly coincide, in EL the E_+ branch follows the polariton dispersion relation [Eq. (1)] less closely than the E_- branch. The EL of E_+ appears to be shifted 75 meV above the fit generated from reflectivity and appears to increase in relative intensity at larger θ. These trends are likely due to residual EL from the poly-TPD hole transport layer that is optically filtered through the E_+ polariton resonance. At larger θ, as E_+ tunes to higher energy, it overlaps with the more intense portion of the poly-TPD luminescence spectrum, with a consequent increase in EL of the E_+ branch, and a blueshift in the observed EL peak of E_+ towards higher energies.

We have shown that it is possible to electrically excite strongly coupled states of light and matter and that electrical excitation preserves the energy levels of the polariton states. Using bilayer assembly, we have achieved Rabi splitting of $\hbar\Omega_i = 265 \pm 15$ meV with 6 nm thick films of active material, and even larger coupling strengths should be achievable with thicker films. Furthermore, by incorporating other optically active molecules within the bilayer assemblies, we expect it will be possible to utilize near-field resonant energy transfer in the strong coupling limit. This could be an enabling step in the design of polariton lasers [19,20] or other cavity QED devices where engineering the occupancy of a particular polariton state [21] is critical for device operation.

The authors thank Professor Rajeev Ram, Tom Liptay, Seth Coe-Sullivan, Conor Madigan, Jen Yu, and Ioannis Kymissis for enlightening discussions and Shoshana Gordon for her technical assistance. We are grateful to the Defense Advanced Research Projects Agency Brown University Optocenter and MIT MRSEC Program of the National Science Foundation under Grant No. DMR 02-13282 for their partial support.

*Department of Electrical Engineering and Computer Science.
†Electronic address: bulovic@mit.edu

[1] P. R. Berman, *Advances in Atomic, Molecular, and Optical Physics*, edited by B. Benderson (Academic Press, Inc., New York, 1994).
[2] M. S. Skolnick, T. A. Fisher, and D. M. Whittaker, Semicond. Sci. Technol. **13**, 645 (1998).
[3] R. J. Thompson, G. Rempe, and H. J. Kimble, Phys. Rev. Lett. **68**, 1132 (1992).
[4] A. Wallraff, D. I. Schuster, A. Blais, L. Frunzio, R. S. Huang, J. Majer, S. Kumar, S. M. Girvin, and R. J. Schoelkopf, Nature (London) **431**, 162 (2004).
[5] C. Weisbuch, M. Nishioka, A. Ishikawa, and Y. Arakawa, Phys. Rev. Lett. **69**, 3314 (1992).
[6] T. Yoshie, A. Scherer, J. Hendrickson, G. Khitrova, H. M. Gibbs, G. Rupper, C. Ell, O. B. Shchekin, and D. G. Deppe, Nature (London) **432**, 200 (2004).
[7] J. P. Reithmaier, G. Sek, A. Loffler, C. Hofmann, S. Kuhn, S. Reitzenstein, L. V. Keldysh, V. D. Kulakovskii, T. L. Reinecke, and A. Forchel, Nature (London) **432**, 197 (2004).
[8] D. G. Lidzey, D. D. C. Bradley, M. S. Skolnick, T. Virgili, S. Walker, and D. M. Whittaker, Nature (London) **395**, 53 (1998).
[9] J. McKeever, A. Boca, A. D. Boozer, J. R. Buck, and H. J. Kimble, Nature (London) **425**, 268 (2003).
[10] M. Saba *et al.*, Nature (London) **414**, 731 (2001).
[11] C. Monroe, Nature (London) **416**, 238 (2002).
[12] H. Fukumoto and Y. Yonezawa, Thin Solid Films **329**, 748 (1998).
[13] M. Vanburgel, D. A. Wiersma, and K. Duppen, J. Chem. Phys. **102**, 20 (1995).
[14] This value is derived from a T-matrix model of the surface reflectance and transmission data of the uncoupled J aggregate peak versus film thickness.
[15] P. A. Hobson, W. L. Barnes, D. G. Lidzey, G. A. Gehring, D. M. Whittaker, M. S. Skolnick, and S. Walker, Appl. Phys. Lett. **81**, 3519 (2002).
[16] Integrating the aqueous PDAC/TDBC bilayers into the RC-OLED structure required cross-linking the spin-cast poly-TPD layer before immersion into the PDAC/TDBC solutions and then drying the structure before thermally evaporating the BCP and patterned metal cathode layers.
[17] A. Kavokin, G. Malpuech, and B. Gil, MRS Internet J. Nitride Semicond. Res. **8**, 1 (2003).
[18] We refer to such an OLED as uncoupled, even though it may exhibit weak microcavity effects due to the half-cavity consisting of metal and ITO electrodes. (See, for example, Bulović *et al.* [22].)
[19] H. Deng, G. Weihs, C. Santori, J. Bloch, and Y. Yamamoto, Science **298**, 199 (2002).
[20] F. P. Laussy, G. Malpuech, A. Kavokin, and P. Bigenwald, Phys. Rev. Lett. **93**, 016402 (2004).
[21] A. Imamoglu, R. J. Ram, S. Pau, and Y. Yamamoto, Phys. Rev. A **53**, 4250 (1996).
[22] V. Bulović, V. B. Khalfin, G. Gu, P. E. Burrows, D. Z. Garbuzov, and S. R. Forrest, Phys. Rev. B **58**, 3730 (1998).